



High performance activated carbon for benzene/toluene adsorption from industrial wastewater

Natalia G. Asenjo*, Patricia Álvarez, Marcos Granda, Clara Blanco, Ricardo Santamaría, Rosa Menéndez

Instituto Nacional del Carbón (CSIC), c/Francisco Pintado Fe, 26–33011 Oviedo, Spain

ARTICLE INFO

Article history:

Received 27 April 2011

Received in revised form 15 June 2011

Accepted 26 June 2011

Available online 1 July 2011

Keywords:

Activated carbon

Benzene

Toluene

Adsorption

Kinetics

ABSTRACT

A coal-tar-derived mesophase was chemically activated to produce a high surface area ($\sim 3200 \text{ m}^2/\text{g}$) carbon with a porosity made up of both micropores and mesopores. Its adsorption capacities were found to be among the highest ever reported in literature, reaching values of 860 mg/g and 1200 mg/g for the adsorption of benzene and toluene, respectively, and 1200 mg/g for the combined adsorption of benzene and toluene from an industrial wastewater. Such high values imply that the entire pore system, including the mesopore fraction, is involved in the adsorption process. The almost complete pore filling is thought to be due to the high relative concentrations of the tested solutions, resulting from the low saturation concentration values for benzene and toluene, which were obtained by fitting the adsorption data to the BET equation in liquid phase. The kinetics of adsorption in the batch experiments which were conducted in a syringe-like adsorption chamber was observed to proceed in accordance with the pseudo-second order kinetic model. The combined presence of micropores and mesopores in the material is thought to be the key to the high kinetic performance, which was outstanding in a comparison with other porous materials reported in the literature.

© 2011 Elsevier B.V. All rights reserved.

1. Introduction

Aromatic compounds such as benzene and toluene are organic compounds that are classified as flammable, toxic, carcinogenic, and/or mutagenic agents [1]. These compounds, however, are often employed in chemical processes as raw materials or even as solvents. The removal of these organic pollutants from the resulting wastewaters is critical to ensure the safety of our water supplies.

The adsorption of organic pollutants by means of porous materials, mainly activated carbons, is a process that has been analysed both in the purification of diluted gas streams [2] and, less often, in the treatment of aqueous solutions [3,4]. Also activated carbon adsorption has been cited by the US Environmental Protection Agency as one of the best available environmental control technologies [5]. In gas phase processes involving diluted streams typical adsorption loads vary in the range of $100\text{--}350 \text{ mg/g}$ for benzene [2] (Silvestre-Albero et al. [6] have claimed the best ever adsorption capacity of 400 mg/g for a KOH activated mesophase pitch-derived activated carbon) and $60\text{--}640 \text{ mg/g}$ for toluene [2]. In gas phase adsorption capacity is thought to be related to the volume of narrow microporosity [6,7] and the presence of oxygen functional groups [8] in the activated carbons, although some authors claim that the

mesopore fraction also contributes to the adsorption of these aromatic species [9]. Both possibilities are compatible if one considers the different degrees of dilution used in these works (200 ppm_v benzene/toluene in [7] and 250 ppm_v benzene in [6] ($p/p_0 < 0.01$) versus $35,000 \text{ ppm}_v$ toluene in [9] ($p/p_0 = 1$)). Naturally at higher adsorbate relative pressures porosity fractions with wider pore diameters will be occupied.

Adsorption in liquid phase may follow a similar pattern to that in gas phase. Jaroniec et al. [10] have proved that the capacity of a given material to adsorb benzene is similar in diluted gas streams and in diluted solutions. It still remains to be proved whether the behaviour of adsorbents under saturated conditions is also similar for both phases (and this constitutes a secondary goal of the present work). Typical adsorption capacities in liquid phase under different conditions are in the range of $12\text{--}230 \text{ mg/g}$ for benzene [4,11–13] and $0.5\text{--}265 \text{ mg/g}$ for toluene [3,12,14–17].

Maximizing the adsorption kinetic rates is another important goal for the economics of the process. In the literature there are not many works devoted to kinetic analyses of benzene or toluene adsorption in aqueous solutions [3,4,11,14–17], and some of these report experiments in which equilibrium is reached only after many hours of batch adsorption. To be able to compare the kinetic performance of different materials a sound approach is to apply a kinetic model and use the derived kinetic parameters (rate constants) in the comparison. Several models are available in literature, such as the Natarajan and Khalaf equation [18], the Elovich equation [19],

* Corresponding author. Tel.: +34 985119090; fax: +34 985297662.
E-mail address: nataliaga@incar.csic.es (N.G. Asenjo).

the power function equation [20], the Lagergren equation [21], the pseudo-second order kinetic model [22], etc. Due to the multiplicity of models available, selection between first-order (i.e. Lagergren model) and second-order models is a good starting point, since both are known to be specific solutions [23] of the widely accepted Langmuir kinetic model [24].

In this work we report on the use of a coal-tar-derived activated carbon for the treatment of an industrial wastewater in which the contaminants present were found to be mainly benzene and toluene. The precursor of the activated carbon used in this study was obtained by the distillation of coal-tar, and has been the object of extensive research by our group [25–27]. Chemical activation of the treated pitch gives rise to activated carbons with very high surface areas (up to $\sim 2700 \text{ m}^2/\text{g}$) and large pore volumes [28]. We report here on the chemical activation of a coal-tar-derived mesophase to produce an activated carbon with high values of surface area and porosity. The main objective of this work is to analyse the performance of this material in the liquid phase adsorption of benzene and/or toluene from synthetic solutions and an industrial wastewater. The total adsorption capacities will be analysed and compared with those reported in the literature for other systems tested under gas and liquid phase conditions. Special emphasis will be placed on a kinetic analysis of the adsorption process, which will serve as a basis for comparison with other adsorbent materials described in the literature. A combination of equilibrium and kinetic analyses allows us to conclude that, under the conditions of this study, the coal-tar-derived activated carbon offers the best results ever reported in terms of adsorption capacity and kinetic rate.

2. Experimental

2.1. Activated carbon

An anthracene oil supplied by a local company was submitted to air-blowing at moderate temperatures, then thermally treated under inert atmosphere at around 400°C and vacuum-distilled to obtain a pitch-like material [25–27,29]. This was then subjected to further heat-treatment at 430°C for 3 h under inert atmosphere and the mesophase part of the pitch was separated via sedimentation [30]. The mesophase was then ground and sieved to a particle size of less than $400 \mu\text{m}$, and mixed with an activating agent (anhydrous KOH) at a weight ratio of 1:5 in an agate mortar. The resulting mixture was then carbonized in an electric furnace at $2.3^\circ\text{C}/\text{min}$ from room temperature to 700°C , under a nitrogen flow rate of $500 \text{ mL}/\text{min}$, and kept at this temperature for 1 h. The carbonized sample was washed thoroughly with a solution of HCl (3 M), and then with hot distilled water until $\text{pH} \approx 7$. Finally the partly agglomerated material was ground and sieved again to a particle size below $400 \mu\text{m}$. Elemental analysis of the resulting activated carbon yielded a carbon content of around 95 wt.% and a total oxygen content below 4 wt.%.

2.2. Textural characterization

The textural characteristics of the samples were analysed by means of N_2 adsorption at 77 K and CO_2 adsorption at 273 K. Both experiments were performed in an ASAP 2020 Micromeritics apparatus using around 100 mg of sample in each experiment. Before the experiments, the sample was outgassed at 350°C for 10 h under vacuum (pressure below 10^{-3} Pa). The following parameters were calculated from the N_2 adsorption isotherm: (1) BET surface area (S_{BET}) in the relative pressure range of 0.05–0.20; (2) total pore volume ($V_{\text{p}}^{\text{N}_2}$) at a relative pressure of 0.99; (3) total micropore volume ($V_{\mu}^{\text{N}_2}$) by means of the Dubinin–Radushkevich equation [31]; (4)

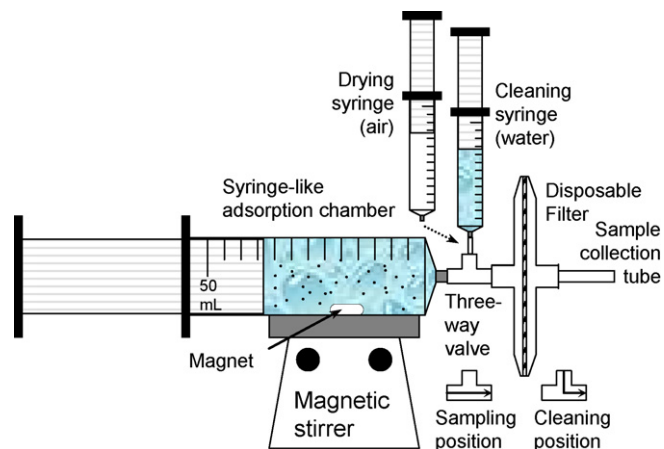


Fig. 1. Syringe-like adsorption chamber for the batch adsorption experiments.

volume of mesopores ($V_{\text{me}}^{\text{N}_2}$) as $V_{\text{p}}^{\text{N}_2} - V_{\mu}^{\text{N}_2}$ and (5) pore size distribution (PSD), characterised by a PSD maximum, $D_{\text{p}}^{\text{N}_2}$, from the density functional theory (DFT) [32]. The volume of narrow micropores ($V_{\mu}^{\text{CO}_2}$) in the activated carbon was obtained from the CO_2 adsorption isotherm.

2.3. Kinetic analysis and equilibrium adsorption. Syringe-like adsorption chamber

For the kinetic experiments a set-up comprising a purpose-designed syringe-like adsorption chamber, a scheme of which is shown in Fig. 1, was employed. The main characteristic of this set-up is that it completely avoids the headspace typically found in other devices and therefore it eliminates the liberation of aromatics to the gas phase. The adsorption medium was placed inside in a 50 mL glass syringe (Fortuna® Optima®) together with a magnet appropriate for non-flat surfaces. The Luer hub of the glass syringe was connected to a three-way valve. A smaller syringe containing water and a disposable paper filter were respectively attached to the other two ends of the valve. During the room-temperature kinetic experiments the adsorption medium was magnetically stirred, the three-way valve being kept for most of this time in the “cleaning” position (Fig. 1). For the sampling which was carried out at regular intervals the three-way valve was turned to the “sampling” position (Fig. 1) and the plunger of the glass syringe was gently pressed to release the required volume of sample (1–2 mL) through the sample collection tube (1/8”). The sample was collected by either a syringe attached to the sample collection tube (for HPLC analysis) or by an UV cuvette (for the UV spectrometry analysis). The active carbon particles carried in the liquid sample were separated using a disposable filter. After sampling, the three-way valve was turned again to the cleaning position; the disposable filter was replaced by a new one; the sampling collection tube was water cleaned by pressing the cleaning syringe and finally it was air dried by means of the drying syringe. It was found that this sampling procedure made it possible to maintain the same carbon-particle mass to liquid volume in the glass syringe throughout the kinetic analysis. Four different aqueous solutions were analysed: (i) synthetic aqueous solutions of benzene (190–210 ppm), (ii) toluene (175–225 ppm), (iii) a mixture of both (175–225 ppm each) and (iv) an industrial wastewater from a local chemical company containing a mixture of benzene ($\sim 120 \text{ ppm}$) and toluene ($\sim 120 \text{ ppm}$), together with trace amounts of chloroform. In all the experiments a liquid volume of 50 mL containing variable loads of active carbon particles (5–30 mg) was employed. The collected liquid samples were analysed by two different methods. The mixed component solutions were analysed by means of High Performance

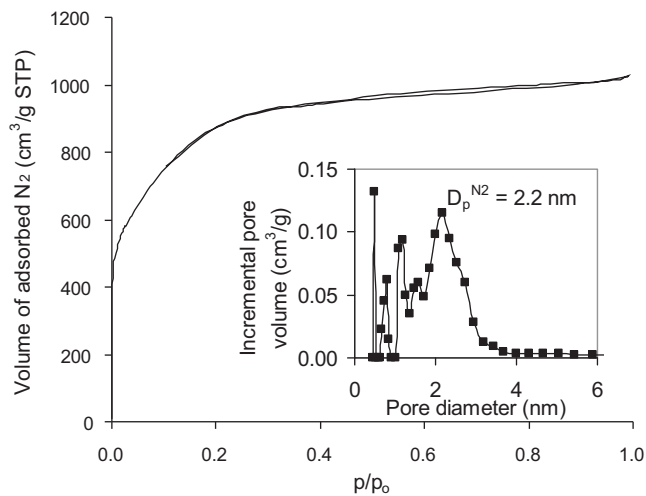


Fig. 2. Nitrogen adsorption isotherm and pore size distribution (inset) of the coal-tar-derived activated carbon.

Liquid Chromatography (HPLC) using an Agilent 1100 series apparatus. The column temperature was set at 27 °C and a UV detector was set to operate at 252.16 nm. Liquid flow rates of 1 mL/min were used in the HPLC column (Agilent Eclipse XDB-C8), the mobile phase being composed of 80% acetonitrile and 20% water. The single component solutions were analysed by means of an UV spectrometer (Shimadzu UV-1800) at wavelengths of 254 nm (benzene) and 268 nm (toluene). The amount of benzene and toluene adsorbed on the activated carbon at a given time, b_t , was evaluated as:

$$b_t = \frac{(C_0 - C_t)}{(W/V)} \quad (1)$$

where C_0 and C_t are the respective concentrations of adsorbate in solution at time zero and time t , and W/V represents the dosage of adsorbent (W , the mass of adsorbent and V , the volume of solution).

The amount of benzene and toluene adsorbed on the activated carbon at equilibrium, b_e , and the concentration of adsorbate in solution at equilibrium, C_e , were obtained from the kinetic data experiments at the longest time (always over 10 min), once the different concentrations had ceased to change. No temporal variation in the concentrations of benzene and toluene was observed during blank experiments performed in the absence of activated carbon.

3. Results and discussion

3.1. Textural properties

Fig. 2 shows the nitrogen adsorption isotherm of the coal-tar-derived activated carbon. The microporous character of the material is visible in the sharp increase in the volume of N_2 adsorbed at low relative pressures, whereas the hysteresis cycle at relative pressures over 0.4 reveals the presence of mesopores, which were absent in previously reported activated carbons of identical origin [28]. This difference is mainly ascribed to the higher relative amount of KOH used for the chemical activation in this study, since it is known that any increase in this parameter causes the pores to open up [33] resulting in a carbon material with a larger BET surface area ($\sim 3200 \text{ m}^2/\text{g}$ versus $2700 \text{ m}^2/\text{g}$ in [28]). As will be explained below, the partial mesoporous character of this material seems to be essential for its high performance in the adsorption of aromatics. The most probable pore diameter of the material ($D_p^{N_2}$), 2.2 nm (inset in Fig. 2), reflects its mesoporous character, with maximum pore diameters of around 4 nm, as evaluated from the N_2 adsorption isotherm. Table 1 shows all of the textural parameters

Table 1

Textural characteristics of the activated carbon obtained from the N_2 (77 K) and CO_2 (273 K) adsorption data.

S_{BET} (m^2/g)	3216
$V_p^{N_2}$ (cm^3/g)	1.59
$V_\mu^{N_2}$ (cm^3/g)	1.01
$V_\mu^{CO_2}$ (cm^3/g)	0.62
$V_{me}^{N_2}$ (cm^3/g)	0.58
$D_p^{N_2}$	2.16

obtained from the analysis of the N_2 and CO_2 adsorption isotherms. As expected, the material has a very high volume of micropores, slightly over $1 \text{ cm}^3/\text{g}$, which is similar to the values obtained by Król et al. [28]. However, the high mesopore volume ($\sim 0.6 \text{ cm}^3/\text{g}$) is a specific characteristic of the material developed here. At the other end of the pore distribution, the narrow microporosity (below 0.7 nm) displays a total volume of $\sim 0.6 \text{ cm}^3/\text{g}$. This is an important parameter since, according to some authors [7,8], the adsorption of benzene and toluene at low concentration in gas phase, which should be similar to that in diluted solutions [10], is performed by the narrow microporosity. If this is the case for the material developed here, then, according to Gurvich's rule [34] the maximum amount of adsorbed benzene can be expected to be around 540 mg/g, similar to that of toluene. On the other hand, if all of the porosity contributes to the adsorption, as occurs in saturated gas streams [9], then the maximum amount of adsorbed benzene or toluene will be around 1400 mg/g.

3.2. Equilibrium adsorption

The equilibrium adsorption data for the different solutions were obtained from the adsorption values at the longest times recorded in the kinetic experiments, once the different concentrations had stabilized. Fig. 3 shows the benzene and toluene adsorption isotherms obtained from the kinetic data recorded at the longest adsorption times for the aqueous solutions. The results for the industrial wastewater (Fig. 3, solid squares) indicate that benzene was adsorbed up to a maximum value somewhere inside the ~ 400 – 500 mg/g range, whereas toluene was simultaneously adsorbed up to a maximum value of $\sim 700 \text{ mg/g}$. Therefore, the maximum combined adsorption of both aromatic species was around 1200 mg/g in the conditions tested in this work. Similar values were obtained for the synthetic mixed solution (Fig. 3, empty squares), indicating that the presence of other substances in the industrial wastewater did not seem to significantly affect the performance of the adsorbent.

For the single component solutions (Fig. 3, solid circles), the maximum amounts of adsorbed benzene and toluene (non-competitive adsorption) reached ~ 870 and $\sim 1200 \text{ mg/g}$, respectively. These results evidence the high adsorption performance of this activated carbon and its ability to remove both molecules from polluted water streams with equal efficiency. Furthermore, these high capacities prove that adsorption is not restricted to the narrow microporosity of the activated carbon but involves the entire pore system.

The high adsorption capacities displayed by this material almost double those of the best performing materials reported in the literature for adsorption in dilute gas streams, whose maximum adsorbed capacities for non-competitive adsorption are around 400 and 640 mg/g for benzene [6] and toluene [2], respectively. All of these materials have a microporous character. Purely mesoporous materials do not seem to be very effective for adsorbing toluene from aqueous solutions. Thus, a mesoporous silica (pore diameter = 20 nm) recently tested for the adsorption of 200 ppm toluene from an aqueous solution [17] showed an adsorption capacity of around 40 mg/g. Only monolithic carbon aerogels, whose pore

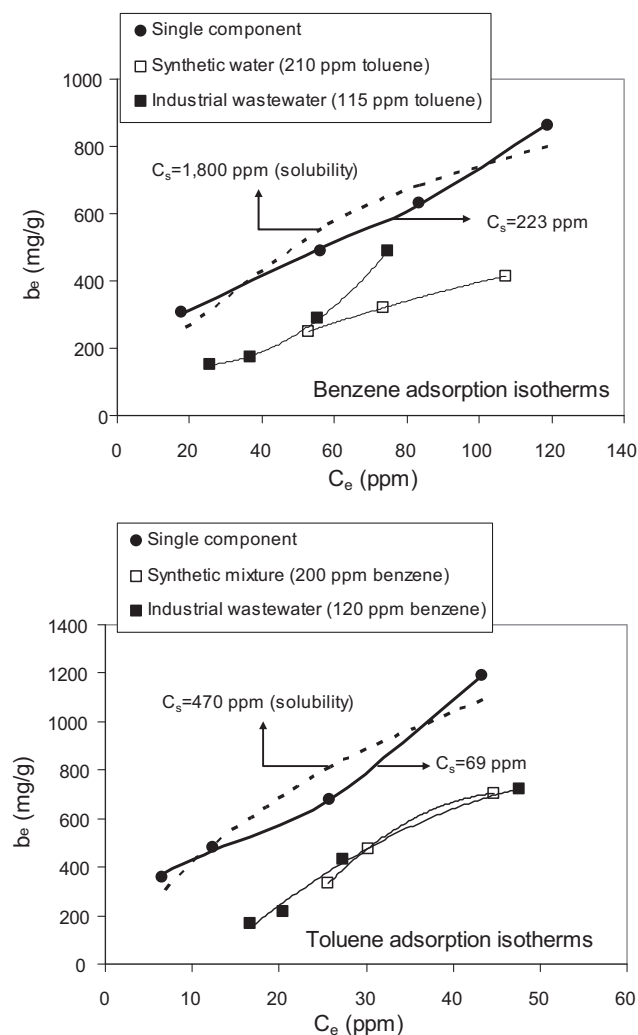


Fig. 3. Benzene and toluene adsorption isotherms for the coal-tar-derived activated carbon analysed in different adsorption media. Lines through the single component points represent fittings to Eq. (2) for C_s values equal to the solubility values of the single components in water at RT (dashed lines) and for C_s values that maximize the R^2 coefficient (continuous lines).

structure was composed of a combination of micropores and mesopores [9], when subjected to an air flow saturated with toluene (3.5 vol.%) displayed similar capacities for toluene adsorption (up to ~ 1180 mg/g) to that of our activated carbon, also characterized by a wide pore distribution from narrow micropores to ~ 4 nm diameter pores (see inset in Fig. 2). Clearly, the high relative pressure employed in the above-mentioned study ($p/p_0 = 1$) [9] made it possible for the pore system of the carbon aerogels to fill up to a greater capacity during the adsorption process.

By extrapolating these results to the liquid phase, the use of the entire porosity of the adsorbent used in this study might imply high values of the relative concentrations of benzene and toluene in the solutions employed in this work. The relative concentration (C_e/C_s , in which C_s is the saturation concentration) of the liquid system should therefore be defined, just as the relative pressure is defined for gas phase adsorption. In a recent critical approach to the use of the BET equation in liquid phase [35], the authors pointed out that in many works the saturation concentration in liquid phase, which is equivalent to saturation pressure in gas phase, is considered to be equal to the solubility of the adsorbate under the conditions being tested. The RT solubility of benzene in water is $S = 1800$ ppm whereas that of toluene is $S = 470$ ppm. Thus, if C_s is made to be

equal to S , the maximum relative concentrations (C_e/C_s) inferred from Fig. 3 are around 0.07 and 0.09 for benzene and toluene, respectively. These values suggest that the solutions used in the present work are diluted at equilibrium, and therefore only the microporosity of the adsorbents should have been filled, contrary to what was experimentally observed. The same authors [35] concluded that the saturation concentration should not be made equal to the solubility concentration but to a much lower value, because saturation of the adsorbent takes place before the solubility concentration is reached. Consequently, the saturation concentration should not take the form of a constant in the BET equation. This assumes the classical form for gas phase adsorption, where liquid phase concentrations are substituted for gas pressures:

$$\frac{C_e/C_s}{b_e(1 - C_e/C_s)} = \frac{1}{b_m c} + \left(\frac{c-1}{b_m c}\right) \left(\frac{C_e}{C_s}\right) \quad (2)$$

where b_m is the monolayer adsorption capacity of the adsorbent and c is a constant that is equivalent to K_S/K_L (K_S being the equilibrium constant of adsorption for the first layer and K_L the equilibrium constant of adsorption for the upper layers).

By applying these assumptions, theoretical adsorption curves can be obtained. As an example Fig. 3 shows the fitting of Eq. (2) to the adsorption curves for the single components in two different cases; (a) where $C_s = S$ and (b) where C_s is a variable that is modified to maximize the value of R^2 . As can be seen, the fitting when $C_s = S$ is clearly unsatisfactory and offers incongruent results, as shown in Table 2. Thus, the monolayer adsorption capacity of the activated carbon in the case of toluene is 1620 mg/g, a value that exceeds the maximum adsorption capacity of the material according to Gurvich's rule, i.e. ~ 1400 mg/g. However, when C_s is adjusted to maximise R^2 , the fittings are acceptable. Even though the number of fitted data points might appear to be insufficient, these fittings offer congruent values (Table 2: b_m values within the expected range and similar c values for benzene and toluene). By applying the C_s values obtained in this case, the relative concentrations for the highest values of adsorption capacity become 0.53 and 0.63 for benzene and toluene, respectively. Thus, in terms of the adsorption isotherm, the liquid phase equilibria take place at relatively high values of relative concentration, making the adsorption of aromatics in liquid phase more similar to that in saturated gas streams than to that in diluted gas streams. Consequently almost total occupation of the activated carbon pores can be expected, as our results indeed confirm.

A search of the literature showed that all of the materials tested in liquid phase performed in general less well for benzene (12–230 mg/g [4,11–13]) and toluene adsorption (0.5–265 mg/g [3,12,14–17]) than the activated carbon prepared in this study. This is a consequence either of testing the adsorbents using much lower relative concentrations or of employing materials with much more reduced pore developments.

3.3. Kinetic experiments

Fig. 4 shows the results of all the batch kinetic experiments (left plots: benzene adsorption; right plots: toluene adsorption). In all cases equilibrium was reached in adsorption times of less than 10 min, which demonstrates the high kinetic performance of the coal-tar-derived activated carbon. In order to compare the results obtained in this study with those of other adsorbents reported in the literature, it is necessary to obtain kinetic data that can be used in the comparison. As mentioned in the Introduction section, many models can be used to fit the experimental data [18–22]. Here we will test two adsorption models of first [21] and second order [22] that are known to be specific solutions [23] of the Langmuir kinetic

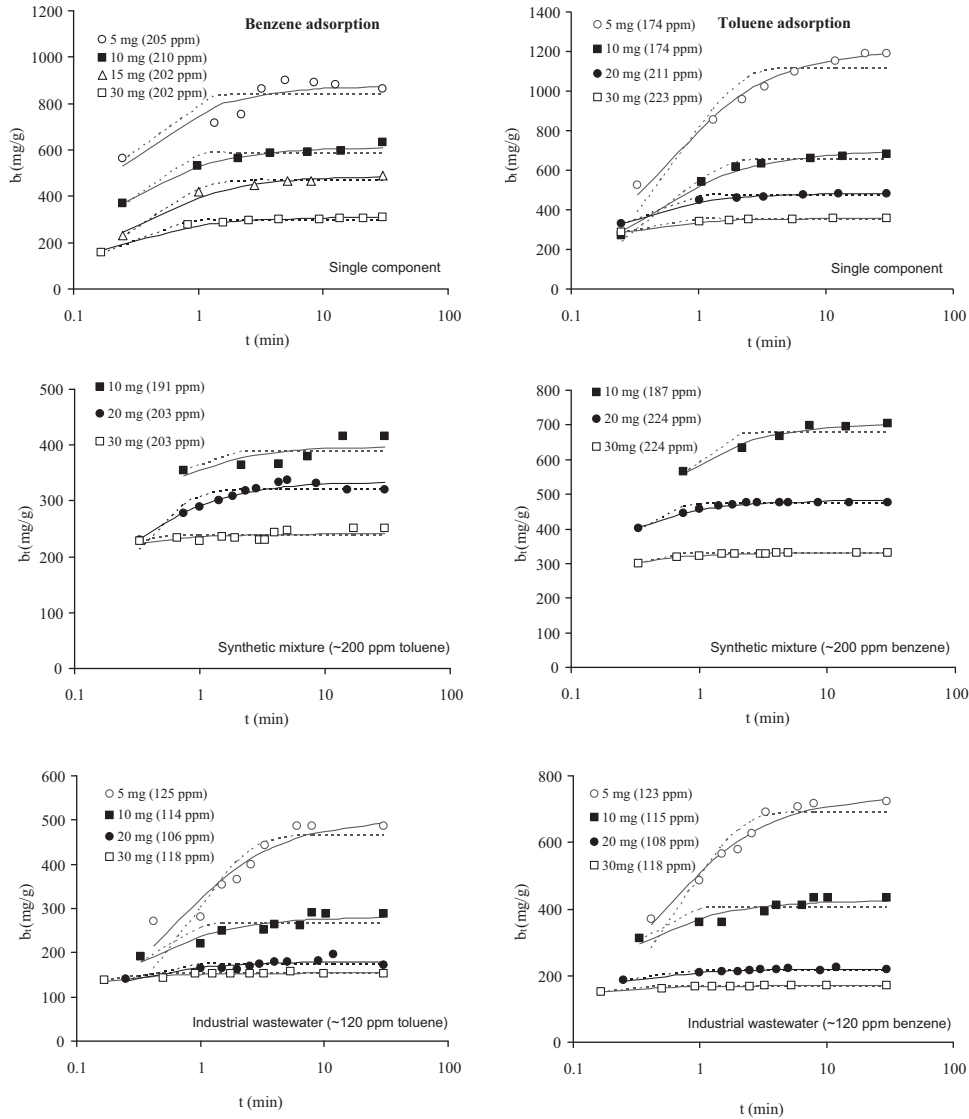


Fig. 4. Variation in the amount of adsorbed benzene (left plots) and toluene (right plots) with time for the coal-tar-derived activated carbon analysed in different adsorption media. The legends indicate the activated carbon mass and the initial adsorbate concentration used in the experiments ($V = 50$ mL). The symbols represent the experimental results. The dashes lines represent the fittings to Eq. (4) (Lagergren model). The continuous lines represent the curve fittings to Eq. (6) (pseudo-second order kinetic model).

model [24]. The first order kinetic model (Lagergren model) can be expressed by the following kinetic equation [21]:

$$\frac{db}{dt} = k_L(b_e - b) \tag{3}$$

By integrating Eq. (3) for the boundary conditions of $t = 0$ up to t , and of $b = 0$ to $b = b_t$, we obtain:

$$b_t = b_e(1 - e^{-k_L t}) \tag{4}$$

The pseudo-second order kinetic model can be represented by the following kinetic expression [22]:

$$\frac{db}{dt} = k_{SE}(b_e - b)^2 \tag{5}$$

Integrating Eq. (5) for the boundary conditions of $t = 0$ up to t , and of $b = 0$ to $b = b_t$, yields:

$$b_t = \frac{k_{SE} b_e^2 t}{1 + k_{SE} b_e t} \tag{6}$$

Table 2
Fitting parameters for the single component isotherms (Fig. 3) to BET Eq. (2).

Single component	C_s (ppm)	R^2	c	b_m (mg/g)	Highest C_e/C_s
Benzene	1800 ^a	0.8749	29.43	1105	0.07
	223 ^b	0.9996	22.88	420	0.53
Toluene	470 ^a	0.7912	15.60	1620	0.09
	69 ^b	0.9998	25.85	455	0.63

^a Solubility values in water at RT.
^b Values obtained from maximizing R^2 .

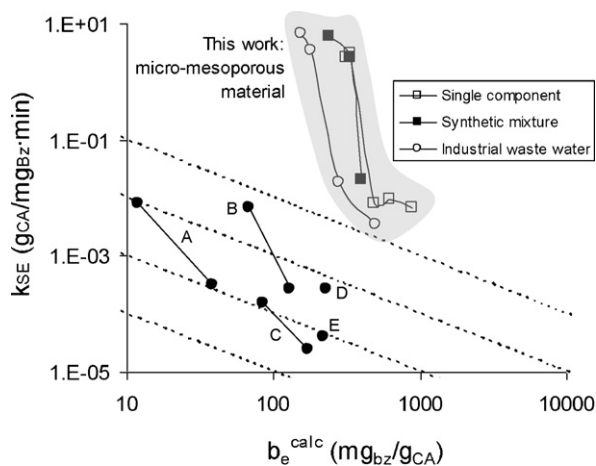


Fig. 5. Variation of the pseudo-second order kinetic rate constant (k_{SE}) with the value of b_e calculated by means of Eq. (6) for the benzene adsorption experiments carried out in this work in different adsorption media (legend), together with the kinetic data obtained from the literature values for the materials described in Table 4.

Parameters k_L , k_{SE} and b_e for both models were obtained by the least squares minimization of the error function $\sum(b_t^{\text{exp}} - b_t^{\text{calc}})^2$, where the b_t^{exp} values are the experimental adsorption data (Fig. 4) and the b_t^{calc} values are those obtained at the same time value by applying Eqs. (4) and (6). The kinetic curves obtained are displayed in Fig. 4 by means of dashed lines (Lagergren model) and continuous lines (pseudo-second order kinetic model). As can be seen, the pseudo-second order kinetic model fits all of the experimental curves more accurately than the Lagergren model. Table 3 shows the average relative errors obtained by fitting the experimental data to both models, corroborating the visual perception of Fig. 4.

Therefore, with the kinetic values obtained from the pseudo-second order kinetic model, it is possible to compare the kinetic performance of the coal-tar-derived activated carbon with that of other materials reported in literature. For the purpose of this comparison the best data representations are those offered by Figs. 5 and 6, which show the variation of k_{SE} with b_e for benzene and toluene adsorption, respectively. Theoretical considerations suggest an inverse relation between these two parameters [23], as has been demonstrated in a number of experimental works [36,37]. The diagonal dashed lines in the figures are pseudo-isokinetic lines of specific k_0 values, k_0 being the pseudo-proportionality constant between k_{SE} and $1/b_e$ ($k_{SE} = k_0/b_e$). As can be seen each consecutive line differs by one order of magnitude. This approximation permits a more logical comparison of the kinetic values, as it takes into account the expected variation of k_{SE} with b_e [36]. Thus, points on the right of a given isokinetic line are thought to represent faster adsorption systems than points on the left of the same isokinetic line. Few published works on batch adsorption of toluene and benzene from aqueous solutions offer kinetic fittings in which the rate constants can be used in the comparison. To overcome this drawback we used a Visual Basic program that can be loaded with bmp-formatted images of the literature kinetic figures reported in pdf documents to extract the numerical values of either b_t or C_t (interchangeable parameters via Eq. (1)) and time [38].

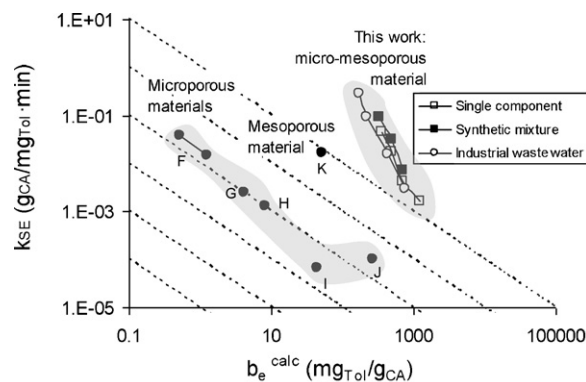


Fig. 6. Variation of the pseudo-second order kinetic rate constant (k_{SE}) with the value of b_e calculated by means of Eq. (6) for the toluene adsorption experiments carried out in this work in different adsorption media (legend), together with the kinetic data obtained from the literature values for the materials described in Table 5.

The extracted data values were fitted to the pseudo-second order kinetic model to yield the different kinetic rate constants displayed in Figs. 5 and 6. Tables 4 and 5 show the works used to construct the figures [3,4,11–17]. The materials used by the different authors together with their main characteristics are also included.

Fig. 5 shows the kinetic parameters of the pseudo-second order kinetic model for the adsorption of benzene. It can be seen that the activated carbon analysed in the present study displays a much better kinetic performance than the materials described in the literature (points A to E), whose main characteristics are shown in Table 4. The effect of the presence of toluene in solution does not affect the benzene adsorption rates of our coal-tar-derived activated carbon; only the rate of adsorption of benzene from the industrial wastewater is slightly lower than the rate of adsorption from the single component solution, probably due to the presence of impurities in the industrial wastewater. This is even less significant in the case of toluene adsorption (Fig. 6) where the kinetic performance of the activated carbon is almost independent of the type of solution analysed. In this figure, the kinetic points obtained for the different materials are grouped according to their main textural properties (Table 5). In principle it is risky to make a kinetic comparison from results obtained in different systems (e.g. different mixing rates) with materials of different particle sizes, as those described in Tables 4 and 5, since in some cases the diffusion resistances can influence the adsorption rates. However, from the pseudo-isokinetic lines, it can be seen that, in general, the adsorption rates of the microporous materials are lower than that of the mesoporous material, and that this is in turn lower than the adsorption rates achieved by the coal-tar-derived activated carbon used in this study, whose porosity is made up of both micropores and mesopores. Marczewski [39] analysed the batch adsorption of nitrobenzene, 4-nitrophenol and 4-chlorophenol from aqueous solutions on mesoporous carbons, and found that these materials displayed much faster adsorption kinetics than microporous carbons of a similar particle size. The results of our work suggest that mesopores act both as a transport and as a concentrating medium and thus enhance the adsorption rate in the micropore system. This could be the explanation for the outstanding performance of the

Table 3
Relative errors ($\%e_r$) for the least square fitting of Lagergren and pseudo-second order kinetic models to the experimental adsorption data displayed in Fig. 4.

$\%e_r$	Benzene adsorption			Toluene adsorption		
	Single component	Synthetic water	Industrial wastewater	Single component	Synthetic water	Industrial wastewater
Lagergren model	0.18 ± 5.28	-0.07 ± 4.26	0.34 ± 8.61	0.77 ± 3.73	-0.02 ± 2.02	0.21 ± 5.69
PSOK model	-0.28 ± 3.80	-0.09 ± 3.09	0.01 ± 5.58	-0.16 ± 2.75	-0.01 ± 0.80	0.06 ± 2.68

Table 4

Materials described in the literature whose kinetic constants are displayed in Fig. 5.

Ref. Fig. 5	Ref.	Material	Characteristics
A	[4]	Calgon Filtrasorb 300 (F300) (activated carbon from bituminous coal)	Microporous material. (S_{BET} : 723 m ² /g). Particle size: 1.2–2 mm
B	[11]	Powdered activated carbon, Dong-Yang Carbon, Incheon, Korea	0.027 mm particle size
C	[11]	Granular activated carbon, Dong-Yang Carbon, Incheon, Korea	2 mm particle size
D	[12]	Multiwall carbon nanotubes oxidized with NaOCl	S_{BET} : 1458 m ² /g V_{μ} : 0.33 cm ³ /g
E	[13]	Silylated MCM-41 (hexagonal mesoporous silica)	Mesoporous material. (S_{BET} : 900 m ² /g), D_p = 4.6 nm

Table 5

Materials described in the literature whose kinetic constants are displayed in Fig. 6.

Ref. Fig. 6	Ref.	Material	Characteristics
F	[3]	Granulated activated carbon (Pica)	S_{μ} : 1577 m ² /g, $S_{\text{meso-macro}}$: 574 m ² /g, $V_{\text{meso-macro}}$: 0.11 cm ³ /g
G	[14]	Alginate complex generated by impregnating synthetic zeolite	PAC + Zeolite ((D_p) = 0.42 nm). Particle size: 4 mm
H	[15]	and powdered activated carbon (PAC) into alginate gel bead	
I	[16]	Granulated active carbon (Picafoam)	High surface area, microporous structure, surface oxide groups and inorganic impurities
J	[12]	Multiwall carbon nanotubes oxidized with NaOCl	S_{BET} : 1458 m ² /g V_{μ} : 0.33 cm ³ /g
K	[17]	Hydrophobic silica aerogel granules (TLD-301)	S_{BET} : 600–800 m ² /g D_p : 20 nm. Particle size: 0.7–1.2 mm

coal-tar-derived activated carbon in the adsorption of benzene and toluene from aqueous solutions.

4. Conclusions

The chemically activated carbon prepared in this study combines a high surface area (3200 m²/g) with a combination of micropores and mesopores that makes it highly suitable for the adsorption of aromatics in aqueous phase. Its benzene and toluene adsorption capacities are among the highest ever reported in the literature (860 mg/g for benzene, 1200 mg/g for toluene and 1200 mg/g for a mixture of both molecules in solution). Such high values can only be accounted for if all of the pore fractions are involved in the adsorption, including the mesopore fraction. The extensive pore filling is thought to be due to the high relative concentrations of the tested solutions, resulting from the low saturation concentration values for benzene and toluene, which were obtained by fitting the adsorption data to the BET equation in liquid phase. The adsorption capacities of the activated carbon were similar both for the synthetic mixtures and for the industrial wastewater, which confirms the suitability of this material for use under practical conditions at industrial scale. The kinetics of adsorption in the batch experiments was observed to follow the pseudo-second order kinetic model. The combined presence of micropores and mesopores in the activated carbon is thought to be the key to its high kinetic performance, which can be described as outstanding when compared with other porous materials reported in the literature.

Acknowledgements

The authors thank the Spanish Science and Innovation Ministry (CONSOLIDER INGENIO 2010, Ref. CSD2009-00050) for their financial support. Dr. Patricia Álvarez thanks the Spanish Science and Innovation Ministry for her Ramón y Cajal contract.

References

- [1] H. Hindarso, S. Ismadji, F. Wicaksana, Mudjijati, N. Indraswati, Adsorption of benzene and toluene from aqueous solution onto granular activated carbon, *Journal of Chemical and Engineering Data* 46 (2001) 788–791.
- [2] M.A. Lillo-Ródenas, D. Cazorla-Amorós, A. Linares-Solano, Behaviour of activated carbons with different pore size distributions and surface oxygen groups for benzene and toluene adsorption at low concentrations, *Carbon* 43 (2005) 1758–1767.
- [3] G. Lesage, L. Sperandio, L. Tiruta-Barna, Analysis and modelling of non-equilibrium sorption of aromatic micro-pollutants on GAC with a multi-compartment dynamic model, *Chemical Engineering Journal* 160 (2010) 457–465.
- [4] C. Liang, Y.J. Chen, Evaluation of activated carbon for remediating benzene contamination: adsorption and oxidative regeneration, *Journal of Hazardous Materials* 182 (2010) 544–551.
- [5] F. Derbyshire, M. Jagtoyen, R. Andrews, A. Rao, I. Martin-Gullon, E.A. Grulke, Carbon materials in environmental applications, 27, 1–66, 2000, Ref Type: Serial (Book, Monograph).
- [6] A. Silvestre-Albero, J.M. Ramos-Fernández, M. Martínez-Escandell, A. Sepúlveda-Escribano, J. Silvestre-Albero, F. Rodríguez-Reinoso, High saturation capacity of activated carbons prepared from mesophase pitch in the removal of volatile organic compounds, *Carbon* 48 (2010) 548–556.
- [7] M.A. Lillo-Ródenas, A.J. Fletcher, K.M. Thomas, D. Cazorla-Amorós, A. Linares-Solano, Competitive adsorption of a benzene-toluene mixture on activated carbons at low concentration, *Carbon* 44 (2006) 1455–1463.
- [8] G.Y. Oh, Y.W. Ju, M.Y. Kim, H.R. Jung, H.J. Kim, W.J. Lee, Adsorption of toluene on carbon nanofibers prepared by electrospinning, *Science of The Total Environment* 393 (2008) 341–347.
- [9] F.J. Maldonado-Hodar, C. Moreno-Castilla, F. Carrasco-Marín, A.F. Pérez-Cadenas, Reversible toluene adsorption on monolithic carbon aerogels, *Journal of Hazardous Materials* 148 (2007) 548–552.
- [10] M. Jaroniec, J. Choma, W. Burakiewicz-Mortka, Correlation between adsorption of benzene from dilute aqueous solutions and benzene vapor adsorption on microporous active carbons, *Carbon* 29 (1991) 1294–1296.
- [11] J.W. Choi, N.C. Choi, S.J. Lee, D.J. Kim, Novel three-stage kinetic model for aqueous benzene adsorption on activated carbon, *Journal of Colloid and Interface Science* 314 (2007) 367–372.
- [12] F. Su, C. Lu, S. Hu, Adsorption of benzene, toluene, ethylbenzene and p-xylene by NaOCl-oxidized carbon nanotubes, *Colloids and Surfaces A: Physicochemical and Engineering Aspects* 353 (2010) 83–91.
- [13] D.B. Patel, S. Singh, R. Bandyopadhyaya, Enrichment of benzene from benzene–water mixture by adsorption in silylated mesoporous silica, *Microporous and Mesoporous Materials* 137 (2011) 49–55.
- [14] J.W. Choi, K.S. Yang, D.J. Kim, C.E. Lee, Adsorption of zinc and toluene by alginate complex impregnated with zeolite and activated carbon, *Current Applied Physics* 9 (2009) 694–697.
- [15] S.J. Lee, S.G. Chung, D.J. Kim, C.E. Lee, J.W. Choi, New method for determination of equilibrium/kinetic sorption parameters, *Current Applied Physics* 9 (2009) 1323–1325.
- [16] M. Arora, I. Snape, G.W. Stevens, The effect of temperature on toluene sorption by granular activated carbon and its use in permeable reactive barriers in cold regions, *Cold Regions Science and Technology* 66 (2011) 12–16.
- [17] D. Wang, E. McLaughlin, R. Pfeffer, Y.S. Lin, Aqueous phase adsorption of toluene in a packed and fluidized bed of hydrophobic aerogels, *Chemical Engineering Journal* (2011), doi:10.1016/j.cej.2011.02.014.
- [18] K. Kannan, A. Vanangamudi, Study on removal of chromium (VI) by adsorption on lignite coal, *Indian Journal of Environmental Protection* 11 (1991) 241–245.

- [19] J. Zeldowitsch, Über den mechanismus der katalytischen oxydation von CO an MnO_2 , *Acta Physicochimica URSS* 1 (1934) 364–449.
- [20] S. Goswami, U.C. Ghosh, Studies on adsorption behaviour of Cr(VI) onto synthetic hydrous stannic oxide, *Water SA* 31 (2005) 597–602.
- [21] S. Lagergren, Zur theorie der sogenannten adsorption gelöster stoffe, *Kungliga Svenska Vetenskapsakademiens Handlingar* 24 (1898) 1–39.
- [22] Y.S. Ho, G. McKay, Pseudo-second order model for sorption processes, *Process Biochemistry* 34 (1999) 451–465.
- [23] Y. Liu, L. Shen, From Langmuir kinetics to first- and second-order rate equations for adsorption, *Langmuir* 24 (2008) 11625–11630.
- [24] I. Langmuir, The adsorption of gases on plane surfaces of glass, mica and platinum, *Journal of the American Chemical Society* 40 (1918) 1361–1403.
- [25] P. Álvarez, J. Sutil, R. Santamaría, C. Blanco, R. Menéndez, M. Granda, Mesophase from anthracene oil-based pitches, *Energy and Fuels* 22 (2008) 4146–4150.
- [26] P. Álvarez, M. Granda, J. Sutil, R. Santamaría, C. Blanco, R. Menéndez, A unified process for preparing mesophase and isotropic material from anthracene oil-based pitch, *Fuel Processing Technology* 92 (2011) 421–427.
- [27] J. Bermejo, A.L. Fernández, M. Granda, F. Rubiera, I. Suelves, R. Menéndez, Effects of thermal treatment on the composition and properties of air-blown anthracene oils, *Fuel* 80 (2001) 1229–1238.
- [28] M. Król, G. Gryglewicz, J. MacHnikowski, KOH activation of pitch-derived carbonaceous materials – effect of carbonization degree, *Fuel Processing Technology* 92 (2011) 158–165.
- [29] A.L. Fernández, M. Granda, J. Bermejo, R. Menéndez, Air-blowing of anthracene oil for carbon precursors, *Carbon* 38 (2000) 1315–1322.
- [30] C. Blanco, R. Santamaría, J. Bermejo, R. Menéndez, A novel method for mesophase separation, *Carbon* 35 (1997) 1191–1193.
- [31] M.M. Dubinin, Fundamentals of the theory of adsorption in micropores of carbon adsorbents: characteristics of their adsorption properties and microporous structures, *Carbon* 27 (1989) 457–467.
- [32] N.A. Seaton, J.P.R.B. Walton, N. Quirke, A new analysis method for the determination of the pore size distribution of porous carbons from nitrogen adsorption measurements, *Carbon* 27 (1989) 853–861.
- [33] D. Lozano-Castelló, M.A. Lillo-Ródenas, D. Cazorla-Amorós, A. Linares-Solano, Preparation of activated carbons from Spanish anthracite: I. Activation by KOH, *Carbon* 39 (2001) 741–749.
- [34] L. Gurvich, *Journal of the Russian Physics and Chemistry Society* 47 (1915) 805–827.
- [35] A. Ebadi, J. Soltan Mohammadzadeh, A. Khudiev, What is the correct form of BET isotherm for modeling liquid phase adsorption? *Adsorption* 15 (2009) 65–73.
- [36] B.H. Hameed, I.A.W. Tan, A.L. Ahmad, Adsorption isotherm, kinetic modeling and mechanism of 2,4,6-trichlorophenol on coconut husk-based activated carbon, *Chemical Engineering Journal* 144 (2008) 235–244.
- [37] W. Plazinski, W. Rudzinski, A. Plazinska, Theoretical models of sorption kinetics including a surface reaction mechanism: a review, *Advances in Colloid and Interface Science* 152 (2009) 2–13.
- [38] I. López, T. Valdés-Solís, G. Marbán, An attempt to rank copper-based catalysts used in the CO-PROX reaction, *International Journal of Hydrogen Energy* 33 (2008) 197–205.
- [39] A.W. Marczewski, Kinetics and equilibrium of adsorption of organic solutes on mesoporous carbons, *Applied Surface Science* 253 (2007) 5818–5826.